ESC European Society of Cardiology

Cardiovascular Research (2019) **115**, 1500–1511
doi:10.1093/cvr/cvy310

Anti-Ro52 antibody acts on the S5-pore linker of hERG to chronically reduce channel expression

John Szendrey[1], Shawn M. Lamothe[1], Stephanie Vanner[2], Jun Guo[1], Tonghua Yang[1], Wentao Li[1], Jordan Davis[1], Mala Joneja[2], Adrian Baranchuk[3], and Shetuan Zhang[1]*

[1]Department of Biomedical and Molecular Sciences, Queen's University, 18 Stuart Street, Kingston, ON K7L 3N6, Canada; [2]Division of Rheumatology, Department of Medicine, Kingston General Hospital, Queen's University, Kingston, Canada; and [3]Division of Cardiology, Department of Medicine, Kingston General Hospital, Queen's University, Kingston, Canada

Received 4 April 2018; revised 9 July 2018; editorial decision 11 December 2018; accepted 11 December 2018; online publish-ahead-of-print 13 December 2018

Time for primary review: 28 days

Aims The human *ether-a-go-go*-related gene (*hERG*) encodes the rapidly activating delayed rectifier potassium channel (I_{Kr}). Malfunction of hERG/I_{Kr} is the primary cause of acquired long QT syndrome (LQTS), an electrical disorder of the heart that can cause arrhythmias and sudden death. Patients with autoimmune diseases display a high incidence of LQTS. While dysfunction of hERG channels induced by autoantibodies such as anti-Ro52 may play a role in this pathology, the underlying mechanisms are not well understood. Here, we investigated the acute and chronic effects of anti-Ro52 antibody on hERG channels stably expressed in human embryonic kidney (hERG-HEK) 293 cells as well as I_{Kr} in neonatal rat ventricular myocytes.

Methods and results Using whole-cell patch clamp, western blot analyses, and immunocytochemistry, we found that a 12-h treatment of hERG-HEK cells with patients' sera containing anti-Ro52 autoantibody decreased the hERG current (I_{hERG}) by 32% compared to cells treated with autoantibody-negative patients' sera. Commercial anti-Ro52 antibody at 100 μg/mL did not acutely block I_{hERG}. Instead, a 12-h treatment with anti-Ro52 antibody at a concentration of 4 μg/mL significantly reduced mature hERG protein expression and I_{hERG}. Specifically, anti-Ro52 antibody did not acutely block hERG current but chronically facilitated hERG endocytic degradation. The extracellular S5-pore linker of hERG, which forms the turret of the channel on the outside of the cell, is the target region for anti-Ro52-mediated hERG reduction since its replacement with the analogous region of EAG abolished the anti-Ro52 effect. In neonatal rat ventricular myocytes, 100 μg/mL anti-Ro52 antibody did not acutely block I_{Kr}, but a 12-h treatment of cells with 4 μg/mL anti-Ro52 antibody selectively reduced I_{Kr} and prolonged the action potential duration.

Conclusions Our results indicate that anti-Ro52 antibody acts on the hERG S5-pore linker to chronically decrease hERG expression and current. These findings provide novel insights into hERG regulation and anti-Ro52 antibody-associated LQTS.

Keywords Cardiac electrophysiology • Potassium channels • Anti-Ro52 antibody

1. Introduction

A high incidence of QT interval prolongation and ventricular arrhythmias have been reported in patients with autoimmune diseases such as systemic lupus erythematosus and Sjögren's syndrome.[1–3] A prolonged QT interval on an electrocardiogram (ECG), a reflection of delay in ventricular repolarization, is known as long QT syndrome (LQTS). LQTS predisposes individuals to a polymorphic ventricular tachycardia known as torsades de pointes that can lead to sudden cardiac death due to ventricular fibrillation.[4] LQTS can be either congenital due to mutations in cardiac ion channels, or acquired due to medical conditions or drugs that decrease the rapidly activating delayed rectifier potassium current (I_{Kr}). The cardiac channel that conducts I_{Kr} is encoded by the human *ether-a-go-go* related gene (*hERG*).[5,6] While mechanisms for autoimmune disease-related long QT are not well understood, autoantibodies have been implicated as a cause. To date, the anti-Ro52 autoantibody has received the most attention for its association with QTc prolongation.[7–12] While anti-Ro52 antibody is most commonly found in patients with systemic lupus erythematosus and other autoimmune diseases, it is also present in the general population with reported rates from 0.6% to

* Corresponding author. Tel: (613) 533-3348; fax: (613) 533-6412, E-mail: shetuan.zhang@queensu.ca

2.7%.[13–15] In 2006, Nakamura *et al.*[9] reported a study related to an anti-Ro52 positive female patient who presented with LQTS and torsades de pointes. They demonstrated that application of the patient's serum to a hERG-expressing human embryonic kidney (HEK) 293 cell line reduced hERG expression. They also found that the serum did not acutely block the hERG current (I_{hERG}). This report was contradicted by other publications by Yue *et al.*[11] and Lazzerini *et al.*[12] which showed that purified anti-Ro52 IgG from autoimmune patients directly blocked I_{hERG}. In the present study, we investigated the effects of anti-Ro52 IgG on hERG expressed in HEK cells and I_{Kr} in neonatal rat ventricular myocytes. Using a chimeric channel made between anti-Ro52 antibody-sensitive hERG and insensitive human *ether-a-go-go* (EAG), we show that anti-Ro52 antibody targeted the extracellular S5-pore linker of hERG to chronically reduce hERG expression in the plasma membrane rather than blocking the channel.

2. Methods

2.1 Human serum collection

The study was reviewed and approved by the Queen's University Health Sciences and Affiliated Teaching Hospitals Research Ethics Board (HSREB, #6017982). Patient consents were obtained before commencement of the study which conforms to the principles outlined in the Declaration of Helsinki. Sixteen patients were recruited during their routine visits to the Kingston Health Sciences Centre (KHSC). Five of them were anti-Ro52 positive, six were anti-Ro52 negative but positive for one or more other autoantibodies (dsDNA, SSA/Ro60, SSB, centromere B, Sm RNP, RNP A, anti-Scl-70), and five were negative for all autoantibodies tested. All patients were under the care of the Division of Rheumatology. Patients were first sorted into their appropriate groups after their serum was analysed for the presence of autoantibodies by the BioPlex 2200 ANA Screen with MDSS (Laboratory Reference Centre, Hamilton General Hospital). The ages of the patients were between 47 and 74 years old. Five were male and 11 female. They were not receiving drugs known to interfere with hERG function, and no cardiac arrhythmias were present during the study. These patients were sent for surface 12-lead ECG recordings. Blood was drawn from the patients into red-capped 15 mL BD Vacutainer Serum Tubes. The whole blood samples were centrifuged at 1000 × g for 10 min at room temperature to fractionate the blood so that the serum could be manually extracted. The extracted sera were either immediately used or stored at -80°C. Cell treatments and patch clamp experiments were performed by independent researchers. 0.5 mL of serum from each patient was applied to hERG-HEK cells cultured in 24-well plates for 12 h. Serum was then washed out and cells were subjected to patch clamp analysis performed by researchers who were blinded to the antibody content of each sample.

2.2 Molecular biology

hERG cDNA was provided by Dr Gail Robertson (University of Wisconsin-Madison). *Kv1.5* cDNA was provided by Dr Michael Tamkun (Colorado State University, Fort Collins, CO, USA); *human ether-a-go-go* (*EAG*) cDNA was provided by Dr Luis Pardo (Max-Planck Institute of Experimental Medicine, Göttingen, Germany). bEAG and hERG-EAG S5-pore plasmids (hERG with its S5-pore linker replaced by the bEAG S5-pore linker, hERG-EAGS5P) were obtained from Dr Eckhard Ficker (Rammelkamp Center for Education and Research, MetroHealth Medical Center, Cleveland, OH[16]). hERG S620T mutation was created using overlapping PCR. hERG, Kv1.5, EAG, S620T hERG, hERG-EAGS5P stable cell lines were created using Lipofectamine 2000 (Invitrogen, Burlington, ON) for transfection of their respective plasmids into HEK 293 cells, and using G418 for selection (1 mg/mL) and maintenance (0.4 mg/mL). Various stable cell lines were cultured in Minimum Essential Medium (MEM, Invitrogen) supplemented with 10% foetal bovine serum (FBS), 1× non-essential amino acids, and 1 mM sodium pyruvate (Invitrogen).

2.3 Neonatal rat ventricular myocyte isolation

Experimental protocols used for animal studies were approved by the Animal Care Committee of Queen's University (Approval no. 1633) and performed in conformity with the NIH guidelines (Guide for the Care and Use of Laboratory Animals). Ten to sixteen 1-day-old Sprague-Dawley rats of either sex were decapitated with sharp scissors. Their ventricles were collected, and single cardiomyocytes were isolated using enzymatic dissociation methods as described previously.[17] Cells were cultured in DMEM/F12 medium (Invitrogen) with 10% foetal bovine serum. Cardiomyocytes were cultured on glass coverslips for electrophysiological studies.

2.4 Patch clamp recording method

The whole-cell patch clamp method was used.[17] Details of solution compositions and voltage protocols are provided in the Supplementary material online. Patch clamp experiments were conducted at room temperature (22 ± 1°C).

2.5 Western blot analysis

Whole-cell protein lysates were extracted from stable cell lines in control and treatment groups. Protein concentration was determined using the Bio-Rad DC Protein Assay Kit (Bio-Rad). 15 μg of protein from each sample was loaded and separated on 8.0% polyacrylamide gels for 2 h. Separated proteins were electroblotted overnight at 4°C onto a PVDF membrane. Membranes were blocked using 5% skim milk in 0.1% Tween 20-containing Tris-buffered saline (TBS) for 1 h. Blocked membranes were immunoblotted for 1 h using appropriate primary antibodies. Immunoblotted membranes were then incubated with corresponding horseradish peroxidase (HRP)-conjugated secondary antibodies. Protein signals were detected using an enhanced chemilumescent (ECL) detection kit (GE Healthcare). The BLUeye prestained protein ladder (FroggaBio) was used to identify band sizes. For quantification of western blot data, intensities of proteins of interest in each gel were first normalized to their respective actin intensities; the normalized intensities were then compared to the control and expressed as values relative to the control.

2.6 Immunocytochemistry

For detection of a potential cross-reaction between hERG and anti-Ro52 antibody, live hERG-HEK cells grown on glass coverslips were exposed to medium containing mouse anti-hERGS5P (targeting S5-pore linker of hERG, 4 μg/mL) or rabbit anti-Ro52 antibody (4 μg/mL) for 30 min on ice (0°C). Afterwards, cells were washed and fixed with ice cold 4% paraformaldehyde for 15 min. Alexa Fluor 594-conjugated donkey anti-mouse or donkey anti-rabbit secondary antibody was used to recognize anti-hERG or anti-Ro52 antibody, respectively. To test the hypothesis that anti-Ro52 antibody interacts and is internalized with hERG, we cultured hERG, EAG or hERG-EAGS5P-expressing HEK cells with

rabbit anti-Ro52 antibody (4 μg/mL) for 4 h. The cells were then washed, fixed, and permeabilized. Alexa Fluor 594-conjugated donkey anti-rabbit secondary antibody was used to detect anti-Ro52 antibody. Goat anti-hERG primary antibody targeting the C-terminus (C-20) and Alexa Fluor 488-conjugated donkey anti-goat secondary antibodies were used to detect hERG and hERG-EAGS5P. Cell membranes were stained using Oregon Green 488-conjugated Wheat Germ Agglutinin (WGA, 5 μg/mL).

2.7 Reagents and antibodies

Rabbit anti-Ro52 antibodies from two suppliers, Santa Cruz Biotechnology (catalogue no. sc-20960 and lot number F0503) and Sigma-Aldrich (catalogue no. AV38248 and lot number QC10839), were used in the present study and produced similar results. Mouse anti-hERGS5P antibody was purchased from DI.V.A.L. Toscana S.R.L., Florence, Italy (catalogue no. DT-331). Recombinant human Ro52 (SSA-52/Ro) protein was purchased from Alpha Diagnostic International (San Antonio, TX, USA). Mouse anti-actin antibody (A4700), electrolytes, HEPES, and brefeldin A (BFA, B6542) were purchased from Sigma-Aldrich. Goat anti-hERG (C-20, sc-15968), as well as mouse-anti goat (sc-2354), goat anti-rabbit (sc-2004), and goat anti-mouse (sc-2005) IgG-HRP secondary antibodies were purchased from Santa Cruz Biotechnology. Minimal essential medium (MEM), G418, FBS, Alexa Fluor 488-conjugated donkey anti-goat (A11055), Alexa Fluor 594-conjugated donkey anti-mouse (A21203), and donkey anti-rabbit (A21207) secondary antibodies, as well as Oregon Green 488 conjugated WGA (W6748) were purchased from Thermo Fisher Scientific.

2.8 Statistical analysis

All data are expressed as the mean ± the standard error of the mean (S.E.M.). A one-way ANOVA with Tukey *post hoc* test or two-tailed Student's *t*-test was used to determine statistical significance between the control and test groups. For comparison of I–V data between control and Anti-Ro52, 2-way ANOVA was used with Bonferroni *post hoc* comparison of the data at each voltage to determine statistical significance. A *P*-value of 0.05 or less was considered significant.

3. Results

3.1 Anti-Ro52 antibody-positive human sera chronically reduced I_{hERG}

In order to assess whether anti-Ro52 and other antibodies affect I_{hERG}, sera were collected from 5 patients positive for anti-Ro52, 6 patients negative for anti-Ro52 but positive for other autoantibodies, and 5 patients negative for all autoantibodies. 0.5 mL of serum from each patient was applied to hERG-HEK cells cultured in 24-well plates for 12 h. Serum was then washed out and cells were subjected to patch clamp analysis. Each patient's serum was randomly assigned a number, regarded as a separate sample, and the data on 7–17 cells from each sample were treated as technical replicates (*Figure 1*A*a*). Experimenters were blinded to the patient serum groups until all experiments were completed. Mean of data from each patient serum was then pooled based on patient groups (*Figure 1*A*b*). Cells treated with sera containing anti-Ro52 autoantibody (anti-Ro52) displayed a 32% reduction in I_{hERG} compared to cells treated with sera from autoantibody-negative patients (CTL, $P < 0.01$, *Figure 1*A*b*). I_{hERG} in cells treated with anti-Ro52 sera was smaller than I_{hERG} in cells treated with sera containing autoantibodies other than anti-Ro52 (Other Ab, $P < 0.05$, *Figure 1*A*b*). There was no significant difference in I_{hERG} between cells treated with sera containing autoantibodies other than anti-Ro52 and cells treated with autoantibody negative sera (CTL; NS: Not Significant; *Figure 1*A*b*). We compared the effects of incubating hERG-HEK cells with 2 μg/mL commercial anti-Ro52 antibody and anti-SSB antibody for 12 h. Anti-SSB antibody treatment did not affect I_{hERG} ($P > 0.05$). However, anti-Ro52 antibody

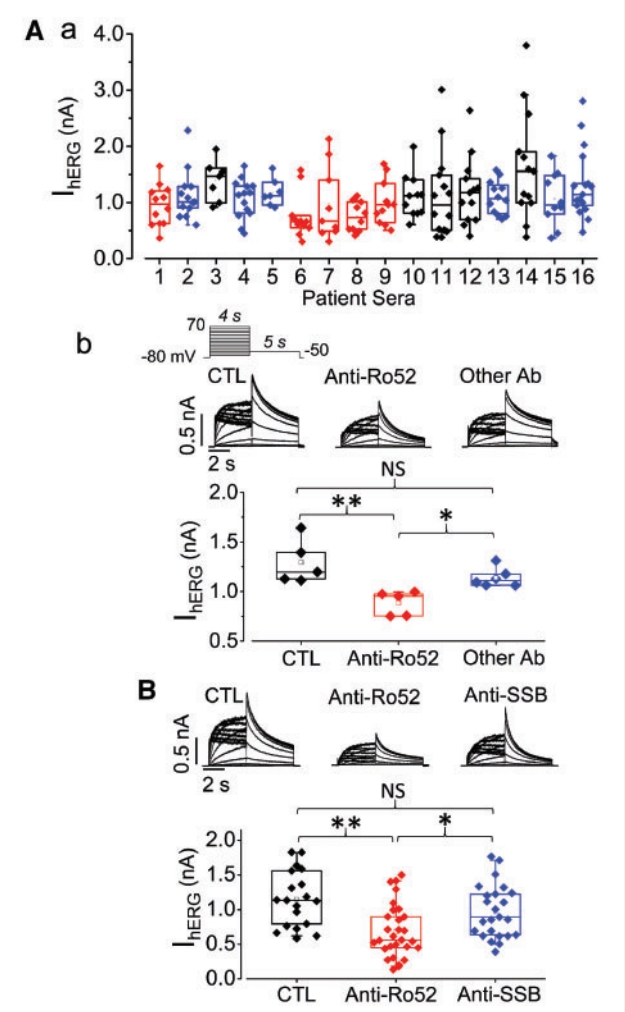

Figure 1 Anti-Ro52 antibody-positive human sera as well as commercial anti-Ro52 antibody chronically reduced I_{hERG}. (*A*) 0.5 mL of serum from each patient was added to culture plates of hERG-HEK cells for 12 h. 7–14 cells were recorded using the voltage protocol shown above the representative currents to determine I_{hERG} from each patient serum treatment. Peak hERG tail current upon -50 mV repolarization after a 50 mV depolarization was used for the amplitude of I_{hERG}. (*a*) Distribution plots of current amplitudes for each serum treatment. Black, control (CTL); Red, anti-Ro52. Blue, other Ab. (*b*) Mean data from each patient were pooled into their respective antibody content groups and summarized beneath representative current traces. (*B*) Effects of treating hERG-HEK cells with 2 μg/mL anti-Ro52 antibody or anti-SSB antibody for 12 h on I_{hERG}. 19–29 cells from each group were examined from three independent experiments. *$P < 0.05$, **$P < 0.01$. One-way ANOVA with Tukey *post hoc* test. NS, not statistically significant.

Table 1 Patient information

Patient (test) tracking number	Male (M) or female (F)	Age	Group[a]	QTc (ms)	History of cardiac events
(1) 0484710	M	68	II	N/A (patient had a pacemaker)	1994 and 1999–acute non-Q wave myocardial infarction and multi-vessel coronary disease 2000–3rd degree AV block; DDDR pacemaker 2001–paroxysmal atrial fibrillation
(2) 1082967	M	64	III	404	2013–premature supraventricular contractions
(3) 0340580	F	68	I	383.3	No history
(4) 0443665	F	48	III	438.2	No history
(5) 0551070	F	64	III	470.2	No history
(6) 0490914	F	62	II	400	2017–premature supraventricular contractions, supraventricular ectopy, paroxysmal atrial tachycardia, ectopic atrial rhythm, and isolated ventricular ectopy.
(7) 1133744	F	56	II	422.3	No history
(8) 0844058	F	54	II	431.5	2011–history of presyncope 2012–intermittent sinus arrhythmia, supraventricular ectopy, and ventricular ectopy.
(9) 0115925	F	58	II	393.6	No history
(10) 0713785	M	68	I	385.3	No history
(11) 0834507	M	74	I	430.1	No history
(12) 0352647	F	47	I	443.1	No history
(13) 0426037	F	59	III	430.2	2013 – occasional premature ventricular complexes
(14) 0527448	M	60	I	361	No history
(15) 0961505	F	68	III	446	No history
(16) 0491346	F	68	III	436	No history

[a]Group.
I. Negative for the presence of all autoantibodies tested.
II. Anti-Ro52 positive.
III. Anti-Ro52 negative but positive for another antibody (dsDNA, SSA/Ro60, SSB, centromere B, Sm RNP, RNP A, Scl-70).

treatment decreased I_{hERG} compared with control (CTL, $P < 0.01$) or anti-SSB antibody treatment ($P < 0.05$, *Figure 1B*).

Acute application of anti-Ro52 positive sera did not affect I_{hERG} (data not shown). Clinical ECG recordings did not identify any patients with prolonged (>480 ms) QTc intervals during the study (*Table 1*). Other details of patient information are summarized in *Table 1*. Notably, a patient in the anti-Ro52 positive group had pre-existing arrhythmia including paroxysmal atrial fibrillation and 3rd degree heart block which was being treated with a DDDR pacemaker. Two additional patients in the anti-Ro52 positive group had ventricular ectopies with one patient possessing a history of presyncope. These incidences were not present in autoantibody-negative patients (*Table 1*).

3.2 Anti-Ro52 antibody did not block I_{hERG} but chronically reduced hERG expression

We investigated the acute effects of anti-Ro52 antibody on I_{hERG} recorded with the whole-cell voltage clamp method in hERG-HEK cells. Rabbit anti-Ro52 antibodies were purchased as 200 μg/mL stock dissolved in Phosphate-Buffered Saline (PBS) from Santa Cruz Biotechnology. We mixed equal amounts of stock solution with the Tyrode (standard bath) solution to achieve a 100 μg/mL concentration for experiments. The control bath solution was also a mixture of PBS and Tyrode solution at a 1:1 ratio. I_{hERG} was elicited using the voltage protocol shown above the current traces every 15 s (*Figure 2A*). The tail current amplitude from each recording was plotted against recording time. Control experiments were performed with a change of bath solution that did not contain antibody. As shown in *Figure 2A*, I_{hERG} in control displayed a rundown to 79 ± 4% of the initial value after 10 min of continuous recording ($n = 9$). I_{hERG} in 100 μg/mL anti-Ro52 antibody-containing solution displayed a similar rundown; after 10 min of continuous recording, I_{hERG} was 76 ± 3% of the initial value ($n = 6$, $P > 0.05$ compared with I_{hERG} in control). To investigate whether anti-Ro52 antibody affects the current–voltage relationship of hERG, families of I_{hERG} were recorded from cells in control or 100 μg/mL anti-Ro52 antibody-containing bath solution (*Figure 2B*). Anti-Ro52 antibody neither reduced the current amplitude nor affected the current-voltage relationships. The activation–voltage (g–V) relationship was obtained by plotting tail currents upon the -50 mV repolarization step against the depolarization voltages. When the g–V curves were fitted to the Boltzmann function, the half activation voltages and slope factors were -14.6 ± 1.9 mV and 6.5 ± 0.3 mV in control cells ($n = 9$), and -16.5 ± 1.7 mV and 6.2 ± 0.2 mV in anti-Ro52 antibody-perfused cells ($n = 9$, $P > 0.05$).

To examine whether anti-Ro52 antibody chronically affects hERG, we cultured hERG-HEK cells for 12 h in medium containing anti-Ro52 antibody at a concentration of 4 μg/mL, which is 25 times less than that used for the acute block experiments. Western blot analysis was used to examine hERG expression in control (CTL) and anti-Ro52 treated cells. Anti-Ro52 reduced the expression of the 155-kDa hERG protein, which represents the mature, fully-glycosylated hERG channel in the plasma

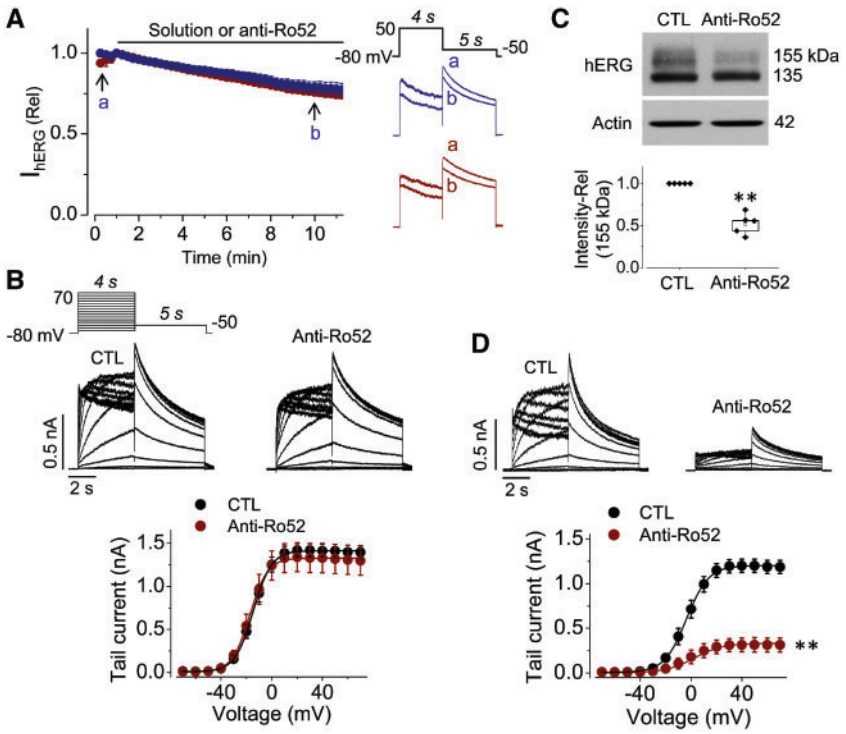

Figure 2 Anti-Ro52 antibody did not acutely block I_{hERG} but chronically decreased mature hERG expression and I_{hERG}. (*A*) Relative I_{hERG} during continuous recordings from cells exposed to control (blue, $n = 9$) or 100 μg/mL anti-Ro52 antibody-containing bath solution (red, $n = 6$). Example current traces at time points of 'a' and 'b' are superimposed. (*B*) Families of hERG currents recorded in cells exposed to control (CTL) or anti-Ro52 antibody (100 μg/mL)-containing bath solution. The activation–voltage relationships for control ($n = 9$ cells) or anti-Ro52 antibody solution ($n = 9$ cells) are shown beneath the current traces. (*C*) Chronic effects of anti-Ro52 antibody (4 μg/mL, 12 h) on the expression of hERG channels. Actin was used as a loading control. The intensity of 155-kDa hERG from anti-Ro52-treated cells was normalized to actin and then compared with that from control cells, and expressed as relative values beneath the western blot image ($n = 5$). $^{**}P < 0.01$ vs. CTL, two-tailed Student's *t*-test. (*D*) Chronic effects of anti-Ro52 (4 μg/mL, 12 h) on I_{hERG}. Representative current traces in control (CTL) and anti-Ro52-treatment along with the activation–voltage relationships are shown ($n = 14$ cells for control (CTL), and $n = 11$ for anti-Ro52 antibody). $^{**}P < 0.01$ vs. CTL at voltages ≥ -10 mV, 2-way ANOVA with Bonferroni *post hoc* comparison at each voltage.

membrane (*Figure 2C*). On the other hand, anti-Ro52 antibody did not affect the 135-kDa hERG protein, which represents the immature, core-glycosylated hERG channels in the endoplasmic reticulum (*Figure 2C*). For patch clamp analysis, after culture without (CTL) or with 4 μg/mL anti-Ro52 antibody for 12 h, hERG-HEK cells were transferred to the recording chamber superfused with the standard (Tyrode) bath solution to record I_{hERG}. Anti-Ro52 antibody treatment significantly reduced I_{hERG} (*Figure 2D*). However, it did not affect the g–V relationship (*Figure 2D*). The half activation voltage and slope factor were -2.9 ± 2.1 mV and 7.2 ± 0.2 mV in control cells ($n = 14$). They were -3.0 ± 2.4 mV and 7.7 ± 0.3 mV in anti-Ro52 antibody-treated cells ($n = 11$, $P > 0.05$). It is noted that a difference exists between the half activation voltages of I_{hERG} for control cells in the acute blockade experiments (*Figure 2B*) and those in chronic experiments (*Figure 2D*). This difference was caused by the reduced Ca^{2+} and Mg^{2+} concentrations in the bath solution used in acute blockade experiments; in acute experiments, the bath solution was a 1:1 mixture of a PBS solution that did not contain Ca^{2+} or Mg^{2+}, and the Tyrode solution that contained 2 mM Ca^{2+} and 1 mM Mg^{2+}. In chronic experiments, the bath solution was the Tyrode solution (compositions of the PBS and Tyrode solutions are described in Supplementary material online).

To investigate the specificity of the anti-Ro52 antibody to hERG, we examined its effects on the hERG-related K^+ channel EAG as well as another cardiac K^+ channel Kv1.5, stably expressed in HEK 293 cells. Cells were cultured in medium without (CTL) or with anti-Ro52 antibody (4 μg/mL) for 12 h. The treatment with anti-Ro52 antibody had no effect on EAG current (I_{EAG}, SI *Figure 1A*) or Kv1.5 current ($I_{Kv1.5}$, SI *Figure 1B*).

3.3 Anti-Ro52 antibody interacts with the hERG extracellular S5-pore linker

We hypothesized that anti-Ro52 antibody added to the culture medium interacts with hERG at an extracellular site of the channel since antibodies are membrane-impermeant. hERG has three extracellular linkers; the S1–S2 linker, the S3–S4 linker, and the S5-pore linker which forms the turret of the channel on the outside of the cell. While the S1–S2 linker contains 24 amino acid residues and the S3–S4 linker contains 4 amino acid residues, the S5-pore linker of hERG is unusually long and contains

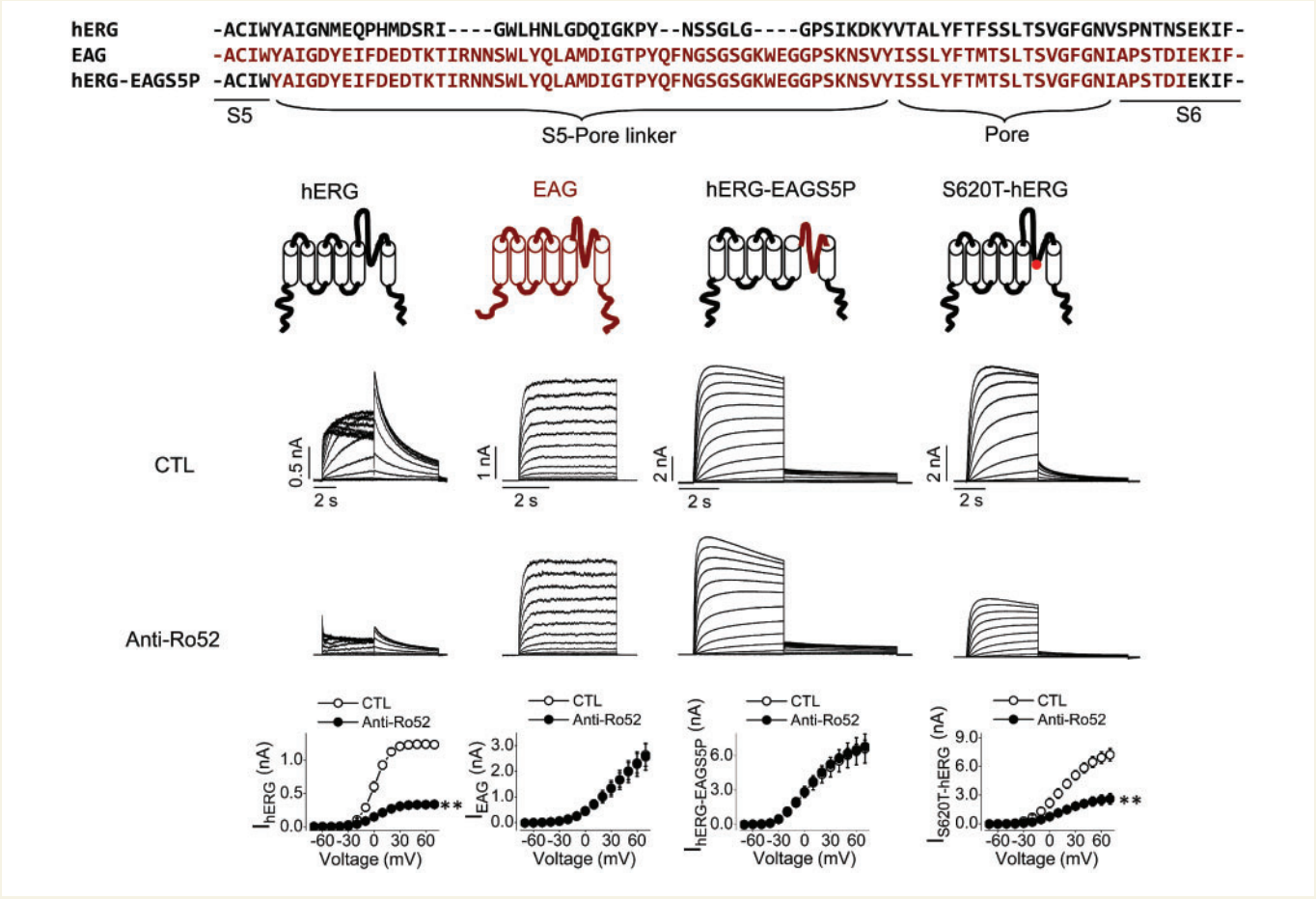

Figure 3 The S5-pore linker is involved in the anti-Ro52 antibody-mediated hERG reduction. Effects of 12-h anti-Ro52 treatment (4 μg/mL) on the currents of hERG, EAG, hERG-EAGS5P, and S620T mutant hERG channels stably expressed in HEK cells. (*Top*) Amino acid sequence alignment of the S5-pore linker and pore region of hERG, EAG and hERG-EAGS5P channels along with the channel topologies. hERG and EAG are illustrated in black and red, respectively. S620T mutation is illustrated by the red dot. (*Middle*) representative current traces of hERG, EAG, hERG-EAGS5P, and S620T-hERG from cells cultured in the absence or presence of anti-Ro52 antibody (4 μg/mL) for 12 h. (*Bottom*) g–V relationships of I_{hERG} ($n = 11$ in CTL, $n = 11$ in anti-Ro52), I–V relationships of I_{EAG} ($n = 6$ in CTL, $n = 8$ in anti-Ro52), $I_{hERG\text{-}EAGS5P}$ ($n = 7$ in CTL, $n = 7$ in anti-Ro52), and $I_{S620T\text{-}hERG}$ ($n = 6$ in CTL, $n = 6$ in anti-Ro52) in control (CTL) and anti-Ro52 antibody-treated cells. $^{**}P < 0.01$ vs. CTL at voltages ≥ -10 mV for hERG and ≥ 10 mV for S620T-hERG, 2-way ANOVA with Bonferroni *post hoc* comparison at each voltage.

43 amino acid residues, whereas the S5-pore linkers of other voltage-gated K^+ channels contain only 10-23 amino acid residues.[18,19] To examine the role of the S5-pore in anti-Ro52 antibody-mediated hERG reduction, we used a chimeric channel in which the S5-pore of hERG was replaced with that of the anti-Ro52 antibody-insensitive EAG channel (hERG-EAGS5P), and tested its response to chronic anti-Ro52 antibody treatment. As shown in *Figure 3*, while a 12-h treatment with anti-Ro52 antibody (4 μg/mL) reduced I_{hERG}, it did not affect I_{EAG}. Interestingly, the hERG-EAGS5P current ($I_{hERG\text{-}EAGS5P}$) was completely resistant to the chronic anti-Ro52 antibody treatment. hERG-EAGS5P current does not inactivate. To confirm that the insensitivity of hERG-EAGS5P to anti-Ro52 antibody was due to the elimination of the antibody interaction site and not due to the absence of inactivation, we tested the effect of anti-Ro52 on the non-inactivating hERG-S620T mutant. Like WT hERG, the current of inactivation-deficient S620T mutant hERG current ($I_{S620T\text{-}hERG}$) was also reduced by anti-Ro52 antibody treatment (*Figure 3*). Thus, we concluded that anti-Ro52 antibody acts on the S5-pore linker to reduce hERG expression.

3.4 Anti-Ro52 antibody does not interact with hERG in an antibody-antigen fashion

It was previously proposed that anti-Ro52 antibody interacted with hERG in an antibody-antigen fashion due to a presumed existence of homology between hERG and Ro52 protein[11,20] (*Figure 4A*). However, in our western blot analyses of proteins extracted from HEK cells (negative control) and hERG-HEK cells, as well as a purchased pure Ro52 protein (positive control), anti-Ro52 antibody recognized Ro52 protein but not hERG (*Figure 4B*, right). On the other hand, an anti-hERGS5P antibody, that targets the S5-pore linker of hERG (catalogue no. DT-331, DI.V.A.L. Toscana S.R.L., Florence, Italy; *Figure 4A*), detected hERG but not anti-Ro52 protein (*Figure 4B*, left). In addition, we stained live hERG-HEK cells with anti-hERGS5P or anti-Ro52 antibody for 30 min on ice. After washes and fixation, appropriate Alexa Fluor 594-conjugated secondary antibodies (red) were used to detect the primary antibodies. While anti-hERGS5P antibody was present on the cell membrane, anti-Ro52 antibody was not detected (*Figure 4C*). Thus, anti-Ro52 antibody does not recognize hERG as an antigen in our experiments.

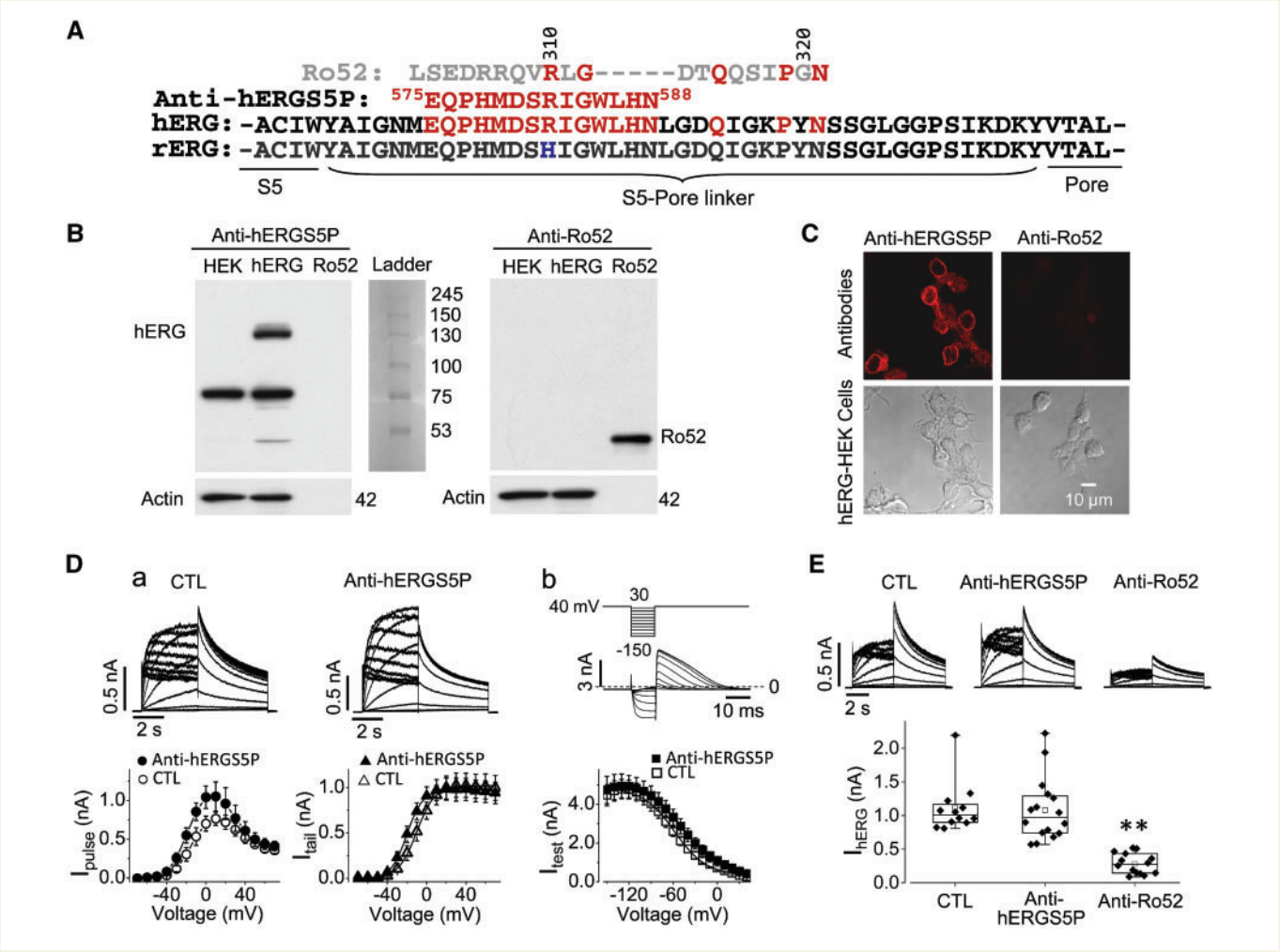

Figure 4 Anti-Ro52 antibody did not recognize hERG as an antigen. (*A*) Amino acid sequence alignment of the S5-pore linker between hERG and rat ERG (rERG) along with the epitope of the anti-hERGS5P antibody as well as a previously presumed homology between hERG and Ro52. (*B*) Western blots showing detection of hERG or Ro52 with anti-hERGS5P or anti-Ro52 antibody. hERG proteins in whole-cell lysate extracted from hERG-HEK cells, as well as pure Ro52 protein were used for detection. Whole-cell lysate extracted from HEK cells was used as a negative control ($n = 5$). (*C*) Confocal images of hERG-HEK cells stained with anti-hERGS5P or anti-Ro52 antibody. Live hERG-HEK cells were exposed to anti-hERGS5P or anti-Ro52 primary antibody on ice for 30 min, fixed, and stained with appropriate secondary antibody ($n = 5$). Scale bar: 10 μm. (*Da*) Representative families of I_{hERG} are shown above the summarized I–V relationships of pulse currents, and g–V relationships of tail currents in the absence (CTL, $n = 8$) and presence of 100 μg/mL anti-hERGS5P antibody ($n = 8$). (*b*) The voltage protocol and an example of current traces along with the summarized steady-state inactivation curves in the absence (CTL, $n = 8$) and presence of 100 μg/mL anti-hERGS5P antibody ($n = 6$). The steady-state inactivation curves were not corrected for the deactivation which was not obvious during 10-ms recovery pulses. (*E*) Effects of 12-h treatments of hERG-HEK cells with anti-hERGS5P antibody (4 μg/mL) or anti-Ro52 antibody (4 μg/mL) on I_{hERG}. Example current traces are shown above the summarized data in each group. $^{**}P < 0.01$ vs. CTL, one-way ANOVA with Tukey *post hoc* test.

Since anti-hERGS5P antibody binds to the hERG S5-pore linker, we examined whether such binding acutely blocks I_{hERG} as previously proposed for anti-Ro52 antibody.[11,20] The anti-hERGS5P antibody came in the DMEM solution with a concentration of 0.3 mg/mL. Thus, we recorded hERG current using DMEM (SI, *Table 1*) as a bath solution. We then changed bath solution to DMEM containing 100 μg/mL anti-hERGS5P antibody and recorded I_{hERG}. Anti-hERGS5P antibody did not acutely block hERG current (SI *Figure 2A*). However, it slightly increased the pulse current while not affecting the maximal tail current amplitude (*Figure 4Da*). The tail current amplitudes were plotted against the depolarizing voltages to obtain g–V curves which were fitted to the Boltzmann function (*Figure 4Da*). Anti-hERGS5P antibody shifted the half activation voltage of the g–V curve from -10.8 ± 3.6 mV ($n = 8$) in control to -20.2 ± 2.5 mV ($n = 8$, $P < 0.05$). It did not affect the slope factor of the g–V curve (7.5 ± 0.5 in control, 7.1 ± 0.3 in anti-hERGS5P antibody, $P > 0.05$).

To examine the effects of anti-hERGS5P antibody on the steady-state inactivation (availability) of hERG channels,[21,22] a voltage protocol shown

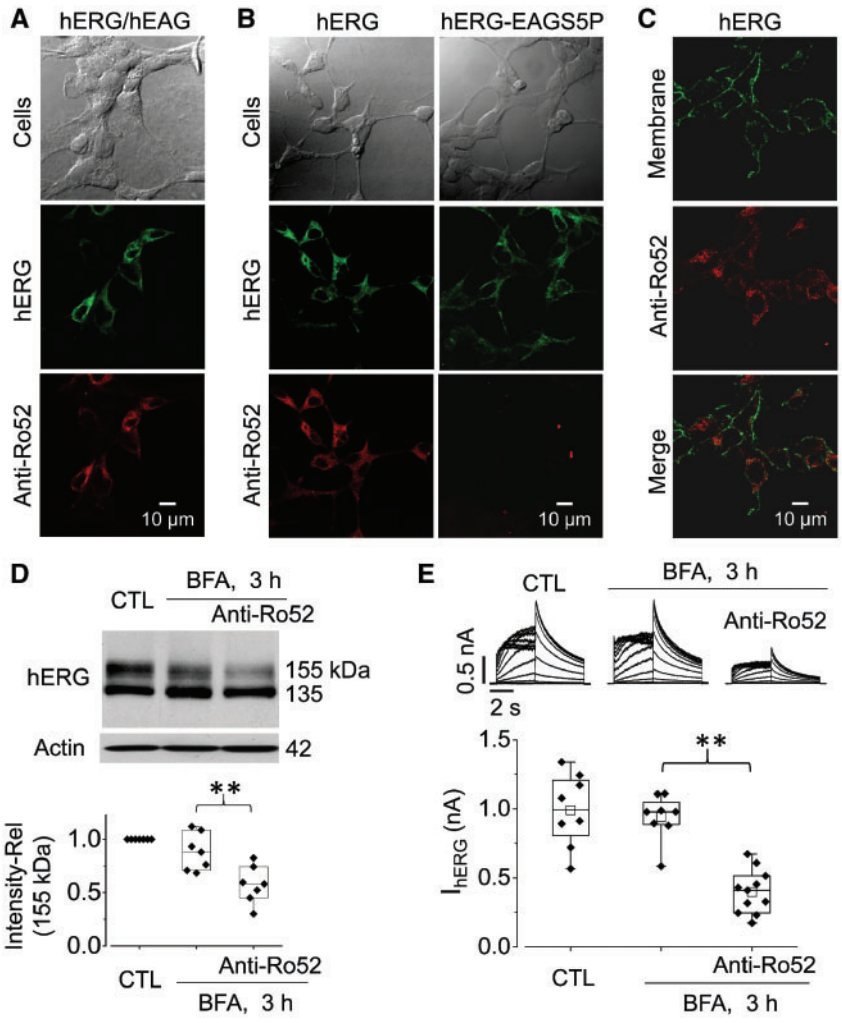

Figure 5 Anti-Ro52 antibody increased the degradation rate of mature hERG channels. (*A*) Detection of anti-Ro52 antibody (red) in hERG- or EAG-expressing HEK cells cultured at a 1:1 mixture with anti-Ro52 antibody (4 μg/mL) for 4 h. hERG-expressing HEK cells are stained green. (*B*) Detection of anti-Ro52 antibody (red) in hERG or hERG-EAGS5P-expressing HEK cells (both stained green) after a 4-h culture with anti-Ro52 antibody (4 μg/mL). (*C*) Localization of anti-Ro52 antibody (red) in hERG-expressing HEK cells. The cell membrane was stained using Oregon Green 488-conjugated WGA. Scale bars in *A*–*C*: 10 μm. (*D*) Effects of anti-Ro52 antibody (4 μg/mL) on hERG expression in BFA (10 μM)-treated hERG-HEK cells. Intensities of the 155-kDa bands from cells treated with BFA without or with anti-Ro52 antibody for 3 h were normalized to that from control (CTL) cells and plotted as relative values beneath the western blot image ($n = 7$). (*E*) Effects of anti-Ro52 antibody (4 μg/mL) on I_{hERG} in BFA (10 μM)-treated hERG-HEK cells. I_{hERG} in cells treated with BFA without or with anti-Ro52 antibody for 3 h, as well as control (CTL) cells was plotted beneath the current traces. $^{**}P < 0.01$, one-way ANOVA with Tukey *post hoc* test.

in *Figure 4Db* was used to elicit hERG currents in the absence or presence of anti-hERGS5P antibody (100 μg/mL). The current amplitudes upon the third pulse to 40 mV were plotted against the test pulses between -150 mV and 30 mV in 10 mV increments to obtain steady-state inactivation curves which were fitted to the Boltzmann function. The half voltage of steady-state hERG inactivation was shifted from -58.1 ± 2.1 mV in control ($n = 8$) to -43.7 ± 4.9 mV ($n = 6$, $P < 0.05$) in the presence of anti-hERGS5P antibody. The slope factor was not changed (22.4 ± 2.1 in control, 23.7 ± 1.6 in anti-hERGS5P antibody, $P > 0.05$).

We further examined the effects of anti-hERGS5P antibody on the voltage dependence of time constants of hERG inactivation, recovery from inactivation, and deactivation. Anti-hERGS5P antibody decreased the time constants of hERG recovery from inactivation at -40 mV; changed the voltage dependence of inactivation time constants (increased at voltages 0–40 mV; decreased at 80–130 mV); and had a trend in increasing the time constants of deactivation (SI *Figure 2B,C*).

We then examined the chronic effects of anti-hERGS5P antibody on hERG channels. hERG-HEK cells were cultured with 4 μg/mL anti-hERGS5P antibody for 12 h. After culture, anti-hERGS5P antibody was washed out and cells were transferred to the perfusion chamber containing standard Tyrode solution for I_{hERG} recording. Chronic treatment with anti-hERGS5P (4 μg/mL) had no effect on I_{hERG} (*Figure 4E*). In contrast, chronic treatment with anti-Ro52 antibody (4 μg/mL) significantly reduced I_{hERG} (*Figure 4E*).

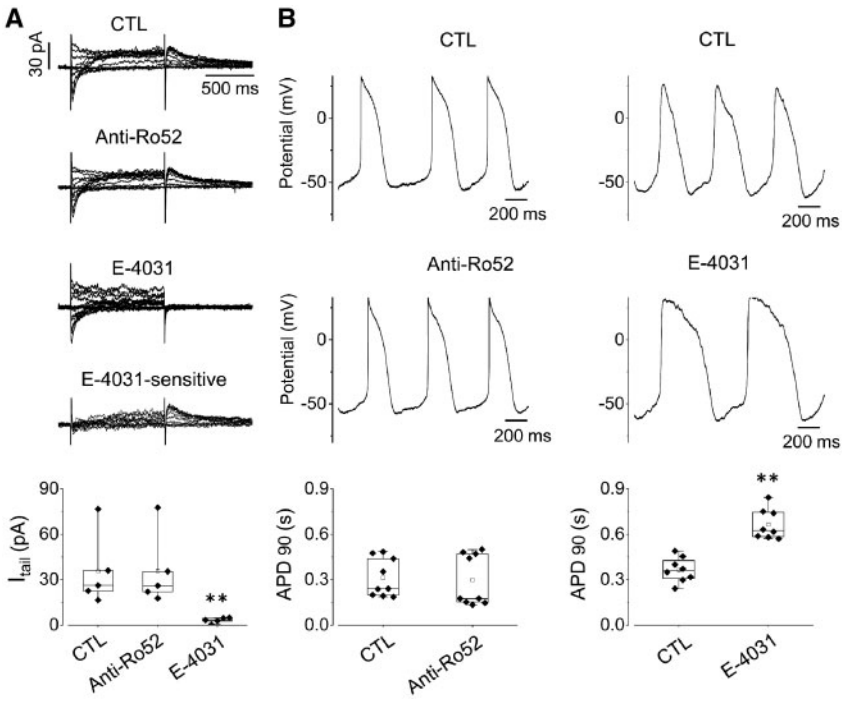

Figure 6 Anti-Ro52 antibody did not acutely block I_{Kr} in neonatal rat ventricular myocytes. (*A*) Potassium current (I_K) was recorded from neonatal rat ventricular myocytes before (CTL) and after anti-Ro52 antibody (100 μg/mL) was added to the bath solution. Anti-Ro52 antibody did not acutely affect I_K. However, the selective I_{Kr} blocker E-4031 (1 μM) eliminated the tail-current of I_K, I_{tail}. Subtraction of I_K in the presence of E-4031 from that in the absence of E-4031 gave the characteristic I_{Kr} (E-4031-sensitive current). I_{tail} in control (CTL), and in the presence of anti-Ro52 antibody or E-4031 are summarized beneath the current traces. $^{**}P < 0.01$ vs. CTL, one-way ANOVA with Tukey *post hoc* test. (*B*) Acute application of anti-Ro52 antibody (100 μg/mL) did not, but E-4031 (100 nM) did, prolong the action potential duration. Action potentials recorded from neonatal rat ventricular myocytes along with the summarized action potential duration at 90% depolarization (APD_{90}) in the absence and presence of anti-Ro52 (100 μg/mL) or E-4031 (100 nM) are shown. $^{**}P < 0.01$ vs. CTL, two-tailed Student's *t*-test.

3.5 Anti-Ro52 antibody increased the degradation rate of mature hERG

Although anti-Ro52 antibody did not recognize hERG in western blot and immunocytochemical assays, it indeed selectively interacted with hERG channels, since the expression of hERG, but not EAG, in HEK cells allowed anti-Ro52 antibody to be internalized after a 4-h culture (*Figure 5A–C*). First, we mixed hERG-HEK cells and EAG-HEK cells in a 1:1 ratio and cultured them with anti-Ro52 antibody (4 μg/mL) for 4 h. Cells were washed, fixed, and permeabilized. Cells were stained with Alexa Fluor 594 (red)-conjugated secondary antibody targeting anti-Ro52 antibody, and stained with an anti-hERG primary antibody and Alexa Fluor 488 (green)-conjugated secondary antibody to identify hERG. Anti-Ro52 antibody was detected in hERG-HEK cells but not in EAG-HEK cells (*Figure 5A*). Second, we compared anti-Ro52 antibody signals between hERG-HEK cells and hERG-EAGS5P-HEK cells, both of which were treated with anti-Ro52 antibody (4 μg/mL) for 4 h. Anti-Ro52 antibody was detected in hERG-HEK cells, but not in hERG-EAGS5P-HEK cells (*Figure 5B*). Third, we stained the cell membrane with Oregon Green 488-conjugated WGA and anti-Ro52 antibodies with the Alexa Fluor 594-conjugated secondary antibody in hERG-HEK cells after a 4-h culture with anti-Ro52 antibody (4 μg/mL). Anti-Ro52 antibody was localized intracellularly (*Figure 5C*).

We hypothesize that anti-Ro52 antibody acts on the S5-pore linker of hERG to promote endocytic degradation of mature hERG channels. To this end, we blocked forward trafficking with brefeldin A (BFA, 10 μM) and examined the effects of anti-Ro52 antibody on hERG expression and I_{hERG}. hERG-HEK cells were cultured in the presence of BFA without (control, CTL) or with anti-Ro52 antibody for 3 h. In the presence of BFA alone, the mature (155-kDa) hERG channel expression as well as I_{hERG} decreased slightly as a result of natural protein degradation. However, presence of anti-Ro52 antibody (4 μg/mL) significantly enhanced the reduction of 155-kDa hERG expression and I_{hERG} (*Figure 5D,E*).

3.6 Anti-Ro52 antibody did not acutely block I_{Kr} but chronically reduced I_{Kr} and prolonged the APD_{90} in neonatal rat ventricular cardiomyocytes

To determine whether the findings we observed in cell lines also occur in native cardiac myocytes, we isolated and cultured ventricular myocytes from neonatal rats. We then acutely applied anti-Ro52 (100 μg/mL) to the bath solution of neonatal ventricular myocytes during patch clamp recordings (*Figure 6A*). We used 5 mM K^+-containing Tyrode bath

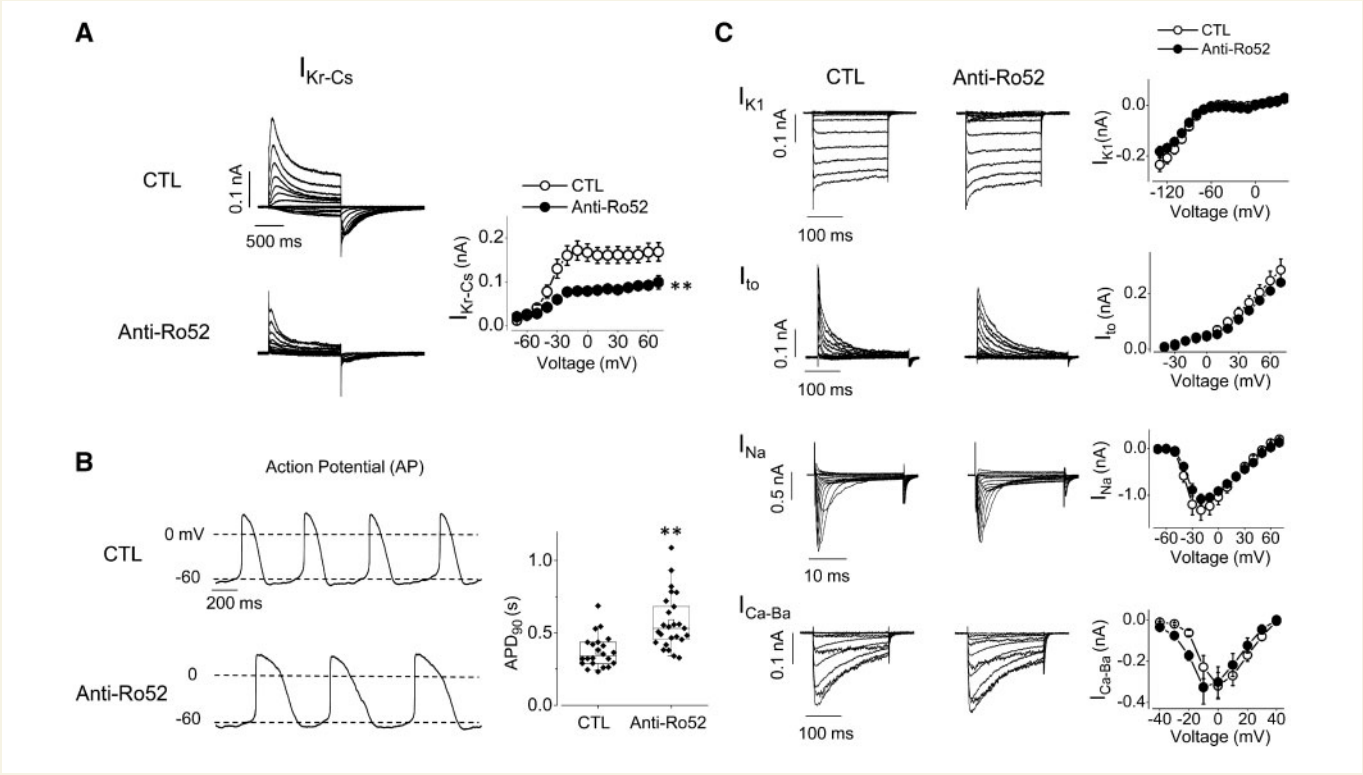

Figure 7 Chronic (12 h) treatment with anti-Ro52 antibody prolonged the APD_{90} and selectively decreased I_{Kr} in neonatal rat cardiomyocytes. (*A*) Effects of anti-Ro52 antibody (4 μg/mL, 12 h) on I_{Kr} isolated by using symmetric 135 mM Cs^+-containing solutions (I_{Kr-Cs}). The inward tail currents upon repolarization to -80 mV were plotted against depolarization voltages in control (CTL, $n = 10$) and anti-Ro52 treated cells ($n = 9$). $^{**}P < 0.01$ vs. CTL at voltages ≥ -30 mV, 2-way ANOVA with Bonferroni *post hoc* comparison at each voltage. (*B*) Effects of anti-Ro52 (4 μg/mL, 12 h) on APD_{90}. APD_{90} values of individual cells from six independent experiments for control (CTL) and anti-Ro52 treatment are shown. $^{**}P < 0.01$ vs. CTL, two-tailed Student's *t*-test. (*C*) Effects of anti-Ro52 (4 μg/mL, 12 h) on inward rectifier K^+ current (I_{K1}, $n = 11$ in CTL, $n = 11$ in anti-Ro52), transient outward K^+ current (I_{to}, $n = 9$ in CTL, $n = 9$ in anti-Ro52), Na^+ current (I_{Na}, $n = 9$ in CTL, $n = 9$ in anti-Ro52), or Ba^{2+}-mediated L-type Ca^{2+} current (I_{Ca-Ba}, $n = 9$ in CTL, $n = 11$ in anti-Ro52). Representative current traces are displayed to the left of their respective summarized I–V relationships.

solution and 135 mM K^+-containing pipette solution to record K^+ current (I_K). We previously demonstrated that the tail current of I_K in neonatal rat ventricular myocytes primarily represents I_{Kr} and that I_{Kr} contributes significantly to repolarization in these cells.[17] Acute application of 100 μg/mL anti-Ro52 antibody did not affect the I_K tail-current (*Figure 6A*). As a positive control, we washed out anti-Ro52 antibody and applied the specific I_{Kr} blocker E-4031 (1 μM), which abolished the tail current of I_K. Subtraction of I_K in the presence of E-4031 from I_K in control revealed the characteristic I_{Kr} (E-4031-sensitive current). These data demonstrated that anti-Ro52 antibody did not block I_{Kr}. We also examined the acute effects of anti-Ro52 treatment on the action potential duration at 90% depolarization (APD_{90}). Anti-Ro52 antibody at a concentration of 100 μg/mL had no effect on APD_{90} when acutely applied during recordings of the action potentials (*Figure 6B*). On the other hand, E-4031 (100 nM) significantly prolonged APD_{90} in neonatal rat ventricular myocytes (*Figure 6B*), demonstrating that I_{Kr} contributes significantly to repolarization in these cells. Due to the nature of our experiments (prepared and cultured cells on Day 1, treated cells on Day 2, and performed recordings on Day 3), the majority of cultured neonatal rat ventricular myocytes displayed automatic firing of action potentials. 100 nM E-4031 also decreased the automatic firing rate (66.3 ± 5.3 beats per minute (b.p.m.), $n = 6$, in control; 41.8 ± 2.7 b.p.m. with E-4031, $n = 6$, $P < 0.01$; *Figure 6B*). While prolongation of the action potential in itself would lead to a slower spontaneous rate due to the delayed time to reach the repolarizing potential, a previous study also showed that I_{Kr} contributes to pacemaker activity; blocking I_{Kr} with E-4031 prolonged APD and slowed the spontaneous rate of Langendorff-perfused mouse hearts.[23]

We then examined the chronic effects of anti-Ro52 antibody on I_{Kr} and APD_{90} in neonatal rat ventricular myocytes. We treated the cultured myocytes with anti-Ro52 antibody (4 μg/mL) for 12 h (*Figure 7*). After treatment, anti-Ro52 antibody was washed away, and patch clamp experiments were performed to compare the amplitude of I_{Kr} (Cs^+-mediated I_{Kr}, I_{Kr-Cs}) and action potential durations between control (CTL) and antibody-treated ventricular myocytes. Anti-Ro52 treatment significantly reduced I_{Kr-Cs} (*Figure 7A*) and prolonged APD_{90} (*Figure 7B*). The spontaneous rate was also slowed down from 67.8 ± 5.4 b.p.m. in control ($n = 10$) to 53.8 ± 3.7 b.p.m. in the anti-Ro52 antibody-treated cardiomyocytes ($n = 15$, $P < 0.05$).

To investigate whether the anti-Ro52 antibody-mediated reduction is specific to I_{Kr}, we examined the effects of anti-Ro52 antibody treatment (4 μg/mL, 12 h) on other currents in neonatal ventricular myocytes. As shown in *Figure 7C*, anti-Ro52 antibody treatment did not affect the inward rectifier K^+ current (I_{K1}), the transient outward K^+ current (I_{to}), Na^+ current (I_{Na}), or L-type Ca^{2+} current (Ba^{2+}-mediated Ca^{2+} channel current, I_{Ca-Ba}).

4. Discussion

LQTS is a dangerous cardiac electrical disorder, which occurs frequently in patients with autoimmune diseases.[1–3] The autoantibody anti-Ro52 has been implicated in the pathogenesis of LQTS in autoimmune patients. Moreover, the clinical relevance of anti-Ro52 antibody extends beyond autoimmune patients,[12] as anti-Ro52 antibody is also found in 0.6–2.7% of the general population.[13–15] A recent study showed that anti-Ro52 antibody was present in 60% of patients who had experienced torsades de pointes.[12] While anti-Ro52 antibody appears to contribute to QT prolongation, the mechanism remains to be determined.[7,8,10,24] In 2015, Yue *et al.*[11] reported that anti-Ro52 antibodies isolated from patients' sera blocked I_{hERG} in hERG-HEK cells. This contradicted a study reported by Nakamura *et al.*[9] in 2007, which demonstrated that the serum of an anti-Ro52 positive patient chronically reduced hERG expression without acutely blocking the channel.

The present study investigated the relationship between autoimmune diseases and LQTS by studying the effects of anti-Ro52 antibody on native I_{Kr} and by generating chimaeras between hERG and the closely related EAG to define the region of the channel that is important for anti-Ro52-mediated current reduction specific to hERG. Our data show that compared to anti-Ro52 negative human sera, anti-Ro52 positive sera chronically decreased I_{hERG} (*Figure 1*). Commercial anti-Ro52 antibody did not block I_{hERG} in hERG-HEK cells (*Figure 2A,B*) or I_{Kr} in cultured neonatal rat ventricular myocytes (*Figure 6*). Rather, it chronically reduced mature hERG expression and I_{hERG} (*Figure 2C,D*), as well as I_{Kr} (*Figure 7*). Furthermore, our data show that replacing the S5-pore linker of hERG with that of EAG abolished the channel sensitivity to anti-Ro52 antibody (*Figure 3*). Thus, we provided evidence to support the notion that anti-Ro52 antibody acts on the S5-pore linker of hERG to trigger hERG internalization (*Figures 3–5*). These data reveal novel insights into anti-Ro52 antibody-associated LQTS.

In addition to hERG expressed in HEK cells, cultured isolated neonatal rat ventricular myocytes were used to study native I_{Kr}. Studying effects on ion channel expression in cardiomyocytes from adult animals is difficult because of the slow protein turnover rate.[17] However, ventricular myocytes from neonatal rats represent a useful tool to study native I_{Kr} function and trafficking.[17,25] While I_{Kr} is not a major K^+ current in adult rats, it is robust and prominent in neonatal rat ventricular myocytes, and displays biophysical, biochemical, and pharmacological properties similar to hERG.[17] As well, the rat clone of ERG (gene for I_{Kr}) is 96% identical to hERG at the amino acid level[26] and can be detected with the anti-hERG antibody.[17] Among the 43 amino acids of the S5-pore linker, 42 of them are identical between human and rat (*Figure 4A*; Uniprot: Q12809 vs. O08962). In addition to K^+-mediated I_{Kr} (*Figure 6A*), Cs^+-mediated I_{Kr} ($I_{Kr\text{-}Cs}$) can be robustly recorded (*Figure 7A*) because Cs^+ blocks other K^+ channels but uniquely permeates through hERG/I_{Kr}.[17,25] Our data show that anti-Ro52 antibody did not acutely block (*Figure 6*), but chronically reduced I_{Kr} and prolonged ventricular action potentials (*Figure 7*).

With regard to how anti-Ro52 antibody decreases I_{hERG}, our data are in line with the work of Nakamura *et al.*[9] but appear to contradict the work from the Boutjdir group.[11,20] The reason for the discrepancy between our results and those from the Boutjdir group[11,20] is unknown. In the studies from the Boutjdir group, they isolated purified IgG containing anti-Ro52 antibodies and affinity purified anti-Ro52 IgG from patients' sera, and demonstrated that these solutions at concentrations of 75 μg/mL and 52 μg/mL, respectively, acutely blocked I_{hERG} in HEK 293 cells stably expressing hERG.[11] As their patients had prolonged QTc values, while those in our experiment did not, it might be possible that the antisera used by the Boutjdir group had a higher affinity for hERG so that they could detect an acute effect.[11] However, with commercial antibodies from two independent suppliers (Santa Cruz Biotechnology, catalogue no. sc-20960, lot number F0503; and Sigma-Aldrich, catalogue no. AV38248, lot number QC10839), our data show that anti-Ro52 antibody at a concentration of 100 μg/mL did not acutely block I_{hERG} or I_{Kr} (*Figures 2* and *6*). Rather, anti-Ro52 antibody at a concentration of 4 μg/mL (25-fold less than the concentration used in the acute blockade experiments) chronically reduced mature hERG expression and I_{hERG} (*Figure 2C,D*), as well as I_{Kr} (*Figure 7*). Yue *et al.* previously proposed that a homology exists between amino acids 302-321 of Ro52 and 574-598 of hERG (*Figure 4A*). This was demonstrated through ELISA, in which patients' anti-Ro52 antibody interacted with a synthesized 31-amino acid peptide corresponding to the pore-forming region (position 572-602) of the hERG channel.[11] However, we examined the effects of an anti-hERG antibody (anti-hERGS5P, DT-331, DI.V.A.L. Toscana S.R.L., Florence, Italy), which targets the amino acid sequence 575-588 (^{575}EQPHMDSRIGWLHN^{588}) of the extracellular S5-pore linker of hERG (*Figure 4A*), on hERG expression and I_{hERG}. Although it is evident that the anti-hERGS5P antibody binds to the hERG channel (*Figure 4B–D*), it neither acutely nor chronically decreased I_{hERG} (*Figure 4*). These observations are in line with data shown in *Figure 4B,C*, arguing against the notion that anti-Ro52 antibody interacts with hERG in an antibody-antigen fashion to block I_{hERG}.

In conclusion, our data show that anti-Ro52 antibody specifically reduces hERG channel density in the plasma membrane and thus I_{hERG}. The anti-Ro52 antibody acts on the S5-pore linker of the channel, resulting in enhanced endocytic degradation of the mature channel. These findings provide novel insights into the regulation of ion channels and mechanisms for autoimmune disease-associated LQTS.

Supplementary material

Supplementary material is available at *Cardiovascular Research* online.

Conflict of interest: none declared.

Funding

This work was supported by the Canadian Institutes of Health Research (PJT 152862 to S.Z.); and Kingston General Hospital Cardiac Program Research Award (to A.B. and S.Z.).

References

1. Sgreccia A, Morelli S, Ferrante L, Perrone C, De Marzio P, De Vincentiis G, Scopinaro F. QT interval and QT dispersion in systemic sclerosis (scleroderma). *J Intern Med* 1998;**243**:127–132.
2. Cardoso CR, Sales MA, Papi JA, Salles GF. QT-interval parameters are increased in systemic lupus erythematosus patients. *Lupus* 2005;**14**:846–852.
3. Goldblatt F, O'Neill SG. Clinical aspects of autoimmune rheumatic diseases. *Lancet* 2013;**382**:797–808.
4. Viskin S. Long QT syndromes and torsade de pointes. *Lancet* 1999;**354**:1625–1633.
5. Trudeau MC, Warmke JW, Ganetzky B, Robertson GA. HERG, a human inward rectifier in the voltage-gated potassium channel family. *Science* 1995;**269**:92–95.
6. Sanguinetti MC, Jiang C, Curran ME, Keating MT. A mechanistic link between an inherited and an acquired cardiac arrhythmia: *hERG* encodes the I_{Kr} potassium channel. *Cell* 1995;**81**:299–307.
7. Lazzerini PE, Acampa M, Guideri F, Capecchi PL, Campanella V, Morozzi G, Galeazzi M, Marcolongo R, Laghi-Pasini F. Prolongation of the corrected QT interval in adult patients with anti-Ro/SSA-positive connective tissue diseases. *Arthritis Rheum* 2004;**50**:1248–1252.

8. Lazzerini PE, Capecchi PL, Guideri F, Bellisai F, Selvi E, Acampa M, Costa A, Maggio R, Garcia-Gonzalez E, Bisogno S, Morozzi G, Galeazzi M, Laghi-Pasini F. Comparison of frequency of complex ventricular arrhythmias in patients with positive versus negative anti-Ro/SSA and connective tissue disease. *Am J Cardiol* 2007;**100**:1029–1034.
9. Nakamura K, Katayama Y, Kusano KF, Haraoka K, Tani Y, Nagase S, Morita H, Miura D, Fujimoto Y, Furukawa T, Ueda K, Aizawa Y, Kimura A, Kurachi Y, Ohe T. Anti-KCNH2 antibody-induced long QT syndrome: novel acquired form of long QT syndrome. *J Am Coll Cardiol* 2007;**50**:1808–1809.
10. Bourre-Tessier J, Clarke AE, Huynh T, Bernatsky S, Joseph L, Belisle P, Pineau CA. Prolonged corrected QT interval in anti-Ro/SSA-positive adults with systemic lupus erythematosus. *Arthritis Care Res* 2011;**63**:1031–1037.
11. Yue Y, Castrichini M, Srivastava U, Fabris F, Shah K, Li Z, Qu Y, El Sherif N, Zhou Z, January C, Hussain MM, Jiang XC, Sobie EA, Wahren-Herlenius M, Chahine M, Capecchi PL, Laghi-Pasini F, Lazzerini PE, Boutjdir M. Pathogenesis of the novel autoimmune-associated long-QT syndrome. *Circulation* 2015;**132**:230–240.
12. Lazzerini PE, Yue Y, Srivastava U, Fabris F, Capecchi PL, Bertolozzi I, Bacarelli MR, Morozzi G, Acampa M, Natale M, El Sherif N, Galeazzi M, Laghi-Pasini F, Boutjdir M. Arrhythmogenicity of anti-Ro/SSA antibodies in patients with torsades de pointes. *Circ Arrhythm Electrophysiol* 2016;**9**:e003419.
13. Peene I, Meheus L, De Keyser S, Humbel R, Veys EM, De Keyser F. Anti-Ro52 reactivity is an independent and additional serum marker in connective tissue disease. *Ann Rheum Dis* 2002;**61**:929–933.
14. Hayashi N, Koshiba M, Nishimura K, Sugiyama D, Nakamura T, Morinobu S, Kawano S, Kumagai S. Prevalence of disease-specific antinuclear antibodies in general population: estimates from annual physical examinations of residents of a small town over a 5-year period. *Mod Rheumatol* 2008;**18**:153–160.
15. Guo YP, Wang CG, Liu X, Huang YQ, Guo DL, Jing XZ, Yuan CG, Yang S, Liu JM, Han MS, Li HX. The prevalence of antinuclear antibodies in the general population of China: a cross-sectional study. *Curr Ther Res Clin Exp* 2014;**76**:116–119.
16. Ficker E, Jarolimek W, Kiehn J, Baumann A, Brown AM. Molecular determinants of dofetilide block of HERG K^+ channels. *Circ Res* 1998;**82**:386–395.
17. Guo J, Massaeli H, Li W, Xu J, Luo T, Shaw J, Kirshenbaum LA, Zhang S. Identification of I_{Kr} and its trafficking disruption induced by probucol in cultured neonatal rat cardiomyocytes. *J Pharmacol Exp Ther* 2007;**321**:911–920.
18. Torres AM, Bansal PS, Sunde M, Clarke CE, Bursill JA, Smith DJ, Bauskin A, Breit SN, Campbell TJ, Alewood PF, Kuchel PW, Vandenberg JI. Structure of the HERG K^+ channel S5P extracellular linker: role of an amphipathic alpha-helix in C-type inactivation. *J Biol Chem* 2003;**278**:42136–42148.
19. Jiang M, Zhang M, Maslennikov IV, Liu J, Wu DM, Korolkova YV, Arseniev AS, Grishin EV, Tseng GN. Dynamic conformational changes of extracellular S5-P linkers in the hERG channel. *J Physiol* 2005;**569**:75–89.
20. Fabris F, Yue Y, Qu Y, Chahine M, Sobie E, Lee P, Wieczorek R, Jiang XC, Capecchi PL, Laghi-Pasini F, Lazzerini PE, Boutjdir M. Induction of autoimmune response to the extracellular loop of the HERG channel pore induces QTc prolongation in guinea-pigs. *J Physiol (Lond)* 2016;**594**:6175–6187.
21. Gianulis EC, Trudeau MC. Rescue of aberrant gating by a genetically encoded PAS (Per-Arnt-Sim) domain in several long QT syndrome mutant human ether-a-go-go-related gene potassium channels. *J Biol Chem* 2011;**286**:22160–22169.
22. Jie LJ, Wu WY, Li G, Xiao GS, Zhang S, Li GR, Wang Y. Clemizole hydrochloride blocks cardiac potassium currents stably expressed in HEK 293 cells. *Br J Pharmacol* 2017;**174**:254–266.
23. Clark RB, Mangoni ME, Lueger A, Couette B, Nargeot J, Giles WR. A rapidly activating delayed rectifier K^+ current regulates pacemaker activity in adult mouse sinoatrial node cells. *Am J Physiol Heart Circ Physiol* 2004;**286**:H1757–H1766.
24. Gordon PA, Rosenthal E, Khamashta MA, Hughes GR. Absence of conduction defects in the electrocardiograms [correction of echocardiograms] of mothers with children with congenital complete heart block. *J Rheumatol* 2001;**28**:366–369.
25. Zhang S. Isolation and characterization of I_{Kr} in cardiac myocytes by Cs^+ permeation. *Am J Physiol Heart Circ Physiol* 2006;**290**:H1038–H1049.
26. Wymore RS, Gintant GA, Wymore RT, Dixon JE, McKinnon D, Cohen IS. Tissue and species distribution of mRNA for the I_{Kr}-like K^+ channel, erg. *Circ Res* 1997;**80**:261–268.